Available online at www.sciencedirect.com
ScienceDirect
International Journal of Heat and Mass Transfer 50 (2007) 1993–2001
International Journal of HEAT and MASS TRANSFER
www.elsevier.com/locate/ijhmt

Single-phase pressure drop and heat transfer characteristics of turbulent liquid nitrogen flow in micro-tubes

S.L. Qi [a], P. Zhang [a,*], R.Z. Wang [a], L.X. Xu [b]

[a] *Institute of Refrigeration and Cryogenics, Shanghai Jiao Tong University, Shanghai 200240, China*
[b] *School of Life Sciences and Technology, Shanghai Jiao Tong University, Shanghai 200240, China*

Received 2 June 2006; received in revised form 20 September 2006
Available online 1 December 2006

Abstract

Experiments have been conducted to investigate the single-phase pressure drop and heat transfer characteristics of liquid nitrogen in four micro-tubes with the diameters of 1.931, 1.042, 0.834 and 0.531 mm. The friction factors are compared with the conventional correlations over a Reynolds number range of 10,000–90,000. The effect of the variable thermal properties of liquid nitrogen, i.e., viscosity and thermal conductivity, on the flow and local heat transfer in the micro-tubes is clarified. The average Nusselt numbers are determined and compared with the correlations for the conventional channels and micro-channels, respectively. It is found that large roughness of the micro-tube causes high friction factor, and the modified Colebrook correlation can well predict the experimental friction factors by using the measured surface roughness. With the increase of liquid nitrogen temperature, the pressure drop decreases as a result of the lower viscosity. Opposite to water, the local heat transfer coefficient of liquid nitrogen flow in the micro-tube drops by 12.5% along the tube. The experimental data show that the average Nusselt numbers for the micro-tubes are higher than those predicted by the correlations for the conventional channels. Taking into account the effect of surface roughness of the micro-tubes on the heat transfer, the modified Gnielinski correlation enables to predict the experimental Nusselt numbers with a mean absolute error (MAE) of 6.4%.

Keywords: Micro-tube; Friction factor; Heat transfer; Liquid nitrogen

1. Introduction

With the development of the miniaturized technologies, mini- and micro-components and systems have been spreading in electronic engineering, biological and medical engineering, space technology and other fields. Some of the components and systems involve the single-phase flow and heat transfer in mini- and micro-channels, about which many research works have been done. Wu and Little [1] investigated the flow characteristics of nitrogen gas flowing through silicon and glass rectangular channels with the hydraulic diameters from 0.045 to 0.165 mm. It was found that the transition from laminar to turbulent flow occurred earlier with the increase of the relative roughness of the surface. Lin et al. [2] measured the pressure drop of refrigerant R-12 in the tubes with diameters of 0.66 and 1.17 mm. The experimental pressure drop was 20% higher than the prediction of Blasius equation. Therefore, they concluded that the relative surface roughness had a remarkable effect on the shear stress at the wall. Experimental investigations by Hsieh et al. [3] also showed a pressure drop higher than that predicted by using the conventional theory. However, the experimental results by Agostini et al. [4] and Yang et al. [5] presented that the experimental friction factors were in good agreement with the conventional correlations.

With respect to the heat transfer in mini- and micro-channels, Wu and Little [6] found that the average Nusselt numbers were higher than those predicted with the conventional correlations for fully developed laminar and turbulent flows. The authors proved that very large relative

* Corresponding author. Tel.: +86 21 34205505; fax: +86 21 34206814.
E-mail address: zhangp@sjtu.edu.cn (P. Zhang).

0017-9310/$ - see front matter © 2006 Elsevier Ltd. All rights reserved.
doi:10.1016/j.ijheatmasstransfer.2006.09.032

Nomenclature

A	cross-section area of tube (m^2)
c_p	specific heat (J/kg K)
D_i	inner diameter of tube (mm)
D_o	outer diameter of tube (mm)
f	friction factor
g	gravitational acceleration (m/s^2)
G	mass flux (kg/m^2s)
h	average heat transfer coefficient (W/m^2 K)
h_x	local heat transfer coefficient (W/m^2 K)
I	electric current through the heater (A)
k	thermal conductivity (W/m K)
k_{ss}	thermal conductivity of tube material (W/m K)
L	tube length (mm)
Nu	Nusselt number
Nu_x	local Nusselt number
p	pressure (kPa)
Δp	pressure drop (kPa)
Pr	Prandtl number
q	average heat flux (W/m^2)
Re	Reynolds number
S	inner surface area of tube (m^2)
T	temperature (K)
U	electric voltage input (V)
V	volume flow rate (m^3/s)
x	distance from the tube inlet (m)
y	distance from the tube wall (m)

Greek symbols

ε	average surface roughness (μm)
μ	viscosity (kg/ms)
ρ	density of liquid phase (kg/m^3)
ρ'	density of vapor phase (kg/m^3)
ζ	local pressure drop coefficient

Subscripts

exp	experimental
f	fluid
i	inner surface of tube
in	inlet of tube
mea	measured
o	outer surface of tube
out	outlet of tube
pred	predicted
ss	stainless steel
w	wall of tube
x	at location x along tube

surface roughness of the micro-channels could improve heat transfer performance. Adams et al. [7] also found that the Nusselt numbers for turbulent flow of water in circular channels with the diameters of 0.76 and 1.09 mm were higher than those for macro-channels. However, the results in Refs. [8,9] showed good agreement between the conventional correlations and the measured data for micro-channels.

The complexity of flow and heat transfer in micro-channels was clarified by the authors [10,11]. They underlined the significant influence of the liquid subcooling, liquid properties, and geometry of micro-channel on the heat transfer and the laminar-to-turbulent transition. More knowledge about flow and convection heat transfer in micro-channels is available in the important reviews [12,13].

From the above literature review, it is evident that large divergence exists for the results of the friction factor and the Nusselt number in mini- and micro-channels; even contrary results are occasionally found. Most researchers conducted the experiments at low Reynolds number regime ($Re < 10{,}000$), and focused on the transition of laminar to turbulent flow. For the higher Reynolds number regime, the experimental data are rarely available. Experimental fluids were mainly water, refrigerant and nitrogen gas, etc., and no data for cryogenic fluids, e.g., liquid nitrogen, are referred.

Recently, in order to realize minimally invasive therapy, mini- and micro-cryogenic surgical apparatus (MCSA) has been successfully applied in cryosurgery, i.e., a procedure that uses extreme low temperature to freeze and destroy the pathological tissue. For example, the MCSA was used in the cosmetology [14] and the treatment of tumors in diverse sites, such as liver [15], uterus [16] and lung [17]. It was also proved to be an effective apparatus for the prostate cryoablation [18]. In the MCSA, liquid nitrogen is usually employed as the working fluid and is supplied to the curative section to maintain its cooling capacity through the micro-tube with the inner diameter of 0.5–2.0 mm. And also with the development of high temperature superconductivity (HTS) science and technology, the superconducting transition temperature has been elevated to around liquid nitrogen temperature range, which enables liquid nitrogen to be used as the coolant for HTS devices, such as Cable-In-Conduit Conductor (CICC) and so on. In the cooling of CICC by forced convection of liquid nitrogen, many small channels with the size in the range of mm or less are usually formed. However, the flow and heat transfer characteristics of liquid nitrogen in the tubes with such sizes (0.5–2.0 mm in diameter), which are crucial for the design and application of the MCSA and the cooling of CICC, are rarely known.

Therefore, the objective of this paper is to investigate the single-phase pressure drop and heat transfer characteristics of liquid nitrogen flowing in the micro-tubes with high Reynolds number ranging from 10,000 to 90,000. The experiments are preformed in the drawing stainless steel circular tubes with the diameters of 1.931, 1.042, 0.834

and 0.531 mm. The friction factor and heat transfer coefficient of the turbulent liquid nitrogen flow are measured and compared with the existing correlations. And the influences of the surface roughness of the micro-tubes and the variations of liquid nitrogen properties on the flow and heat transfer are clarified.

2. Experimental apparatus and procedures

2.1. The test loop

The schematic illustration of the experimental apparatus is shown in Fig. 1. To minimize heat leakage from the ambient, the liquid nitrogen storage tank and test section are installed in a vacuum dewar. Liquid nitrogen is supplied to the test section by the pressurized nitrogen gas from a high-pressure nitrogen gas cylinder. By adjusting the reductor and the valve connected to the nitrogen gas cylinder, the system pressure can be controlled at a required stable state. The system pressure is in the range of 100–900 kPa. Two rows of filters are placed upstream the micro-tube to avoid the frazil and other impurities blocking the flow passage. A valve located at the outlet of the test section is used to control the flow rate. An evaporator immersed in a 20 °C circulated water bath ensures that liquid nitrogen from the test section evaporates completely. Finally, nitrogen gas is exhausted through a vortex flowmeter.

2.2. The test section

The test section is installed vertically in the vacuum dewar, as shown in Fig. 2. The tube and the inlet/outlet flanges are soldered together. Liquid nitrogen flows upward through the micro-tube. To ensure the flow stability, there is a mixing chamber at the inlet and outlet of the test section, respectively. The chamber and test section flange are bonded together with six bolts. Two pressure taps are directly set through the micro-tube wall at the places with a certain distance downstream and upstream the inlet and outlet, and are connected to the absolute pressure transducers. In this way, the local pressure drop caused by the sudden contraction and expansion can be excluded, and the pressure difference is determined

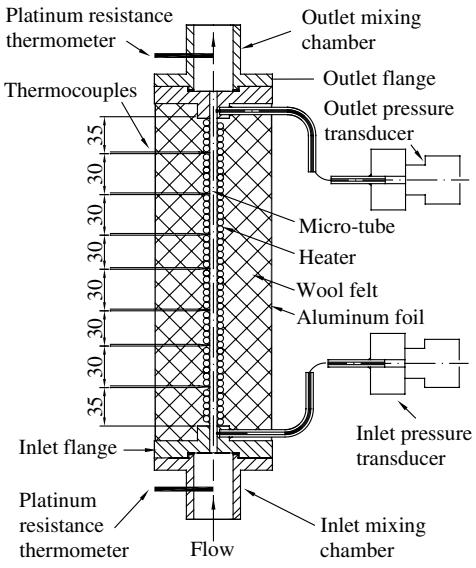

Fig. 2. The schematic illustration of the test section (all dimensions are in mm).

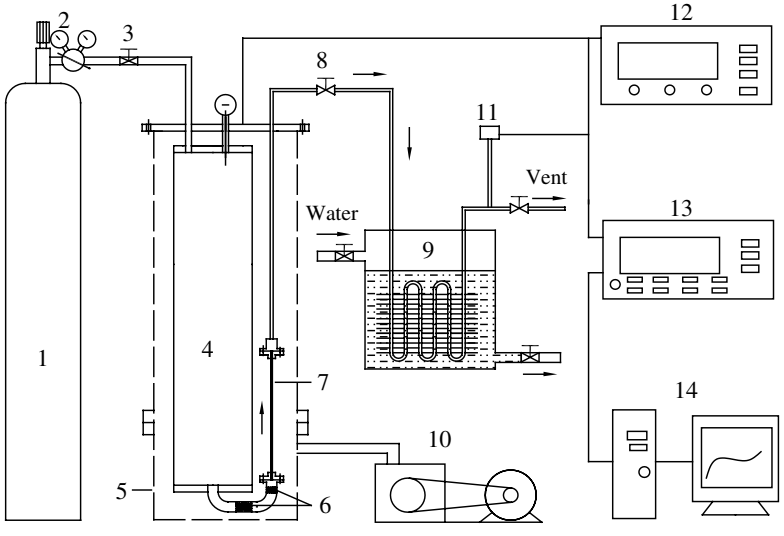

1. Nitrogen gas cylinder
2. Reductor
3. Pressure control valve
4. Liquid nitrogen storage tank
5. Vacuum dewar
6. Filter
7. Test section
8. Flow rate control valve
9. Evaporator
10. Vacuum pump
11. Vortex flowmeter
12. DC power controller
13. Data acquisition device
14. Computer

Fig. 1. The schematic illustration of the experimental apparatus.

Table 1
Dimensions of the micro-tubes

Number	Tube diameter (mm)		Tube length (mm)
	D_i	D_o	
1	1.931	2.912	250
2	1.042	1.638	250
3	0.834	1.238	250
4	0.531	0.842	250

according to the outputs of two pressure transducers. The uncertainty of the pressure drop measurement is within ±0.3 kPa by a standard calibration.

Liquid temperatures at the inlet and outlet of the experimental section are measured by using the platinum resistance thermometers with an accuracy of about ±0.1 K. Seven T-type (copper-constantan) thermocouples with a diameter of 0.1 mm are soldered on the outer surface of the micro-tube to measure the wall temperature. Prior to the installation, all the thermocouples are calibrated by a standard Lakeshore calibration system with an accuracy of about ±0.1 K.

Commercial stainless steel (ss, Type 304) tubes, usually used to fabricate medical injectors, are employed as the test channels. The tube diameter is determined by using a 500× microscope, whose measurement accuracy is ±0.001 mm. Overall, four tubes are tested, and their dimensions are given in Table 1.

The manganin wire with a diameter of 0.18 mm is tightly coiled around the tube as the heater. It should be noted that the wire must be enlaced carefully to avoid contacting with the thermocouples. To ensure the uniformity of heat flux, a thin layer of cryogenic glue is uniformly painted around the tube after the wire is enlaced. The heat flux is adjusted by changing the electric current delivered from the DC power (the maximum power is 360 W). One layer of wool felt with about 15 mm thickness is wrapped around the heater to reduce heat leakage. Outside of the felt layer, there is a layer of aluminum foil used as a radiation shield. Overall heat loss including the heat radiation to the ambient and heat conduction from the ends of the stainless tube is estimated to be less than 5% of the input power. The result is verified by heat balance between the ohmic heat input and the sensible heat increase of the fluid.

2.3. The test procedures

With liquid nitrogen as the working fluid, the cooling process of the whole system is very crucial and usually takes a few hours. Before each experiment, the dewar containing the test section is precooled to about 150 K, and evacuated by a mechanical vacuum pump to 2.0–5.0 Pa. All the data are collected when the experiment reaches a steady state defined in such a way that the pressure drop and the wall temperature fluctuate within ±5% and ±0.1 K, respectively. All the outputs of the thermocouples, electric current and voltage, flowmeter and pressure transducers are recorded by a data logger (Keithley 2700) and stored in a personal computer for further analysis.

3. Data reduction

3.1. Pressure drop

The mass flux of liquid nitrogen, G, can be calculated

$$G = \frac{V\rho'}{A} \tag{1}$$

where ρ' is the density of nitrogen gas. The volumetric flow V is measured by the flowmeter.

In most cases, the measured pressure drop consists of four parts, i.e., friction (Δp_f), local (Δp_l), gravitation (Δp_g) and acceleration (Δp_a) pressure drop components

$$\Delta p_{mea} = \Delta p_f + \Delta p_l + \Delta p_g + \Delta p_a \tag{2}$$

where

$$\Delta p_f = f\frac{G^2}{2\rho}\frac{L}{D_i}; \quad \Delta p_l = \zeta\frac{G^2}{2\rho}; \quad \Delta p_g = \rho g L;$$
$$\Delta p_a = \frac{G^2}{2\rho_{in}}(\rho_{in}/\rho_{out} - 1) \tag{3}$$

and ζ is the local pressure drop coefficient at the inlet and outlet of the tube. For the micro-tubes, however, it is difficult to evaluate ζ because the conventional correlation may not be applicable [5,13]. In the present experiments, the pressure at a certain distance downstream and upstream the inlet and outlet is directly measured, as shown in Fig. 2, which can exclude the local pressure drop caused by the sudden contraction and expansion at the inlet and outlet of the tube. Hence, Δp_l is taken to be zero. The difference between the entrance density (ρ_{in}) and the exit density (ρ_{out}) is very small because of the incompressibility of the liquid nitrogen. Therefore, the acceleration pressure drop component Δp_a is estimated being so small, less than 100 Pa, that it can be neglected in data reduction.

The Darcy friction factor f can be obtained by

$$f = (\Delta p_{mea} - \rho g L)\frac{2\rho}{G^2}\frac{D_i}{L} \tag{4}$$

The Reynolds number is defined as

$$Re = \frac{D_i G}{\mu_f} \tag{5}$$

where μ_f is the liquid viscosity base on the mean fluid temperature.

3.2. Heat transfer

The heat flux is calculated by

$$q = \frac{UI}{S} \tag{6}$$

The inner wall temperature is determined with a correction for the temperature drop over the wall thickness

Table 2
Summary of the uncertainty analysis

Parameter	Uncertainty
Parameter measurement	
Diameter, D (mm)	±0.001
Length, L (mm)	±1.0
Temperature, T (K)	±0.1
Pressure difference, P (kPa)	±0.3
Volume flow rate, V (%)	±2.0
Parameter derived	
Mass flux, G (%)	±2.1
Heat flux, q (%)	±4.0
Reynolds number, Re (%)	±2.1
Friction factor, f (%)	±6.3
Nusselt number, Nu (%)	±7.8

$$T_{w,i} = T_{w,o} - \frac{qD_i \ln(D_o/D_i)}{2k_{ss}} \tag{7}$$

The local heat transfer coefficient is given by

$$h_x = q/(T_{w,i} - T_{f,x}) \tag{8}$$

where $T_{f,x}$, the fluid temperature, is evaluated by the heat balance along the tube

$$T_{f,x} = T_{f,in} + \int_0^x \frac{q \cdot S}{G \cdot A \cdot c_p(x) \cdot L} dx \tag{9}$$

The local Nusselt number is determined base on the local heat transfer coefficient

$$Nu_x = \frac{h_x D_i}{k_{f,x}} \tag{10}$$

Therefore, the average Nusselt number is

$$Nu = \frac{1}{7}\sum_{i=1}^{7} Nu_i \tag{11}$$

The local thermal properties of liquid nitrogen are determined by using the formulas from Ref. [19].

The uncertainties of f and Nu in these experiments can be determined according to the measurement uncertainties of the tube diameter, tube length, volume flow rate, pressure difference and heat flux. All the experimental uncertainties are summarized in Table 2. It can be seen that the uncertainties of f and Nu are no more than 6.3% and 7.8%, respectively.

4. Results and discussion

4.1. Single-phase pressure drop

4.1.1. The pressure drop versus mass flux

The variation of the experimental pressure drop with the liquid nitrogen mass flux is shown in Fig. 3. The pressure drop increases monotonically for all the micro-tubes with the increase of the mass flux. Compared with the results for the conventional channels, the pressure drop through the micro-tubes is very large. For example, the pressure drop through the 0.834 mm tube with a length of 250 mm

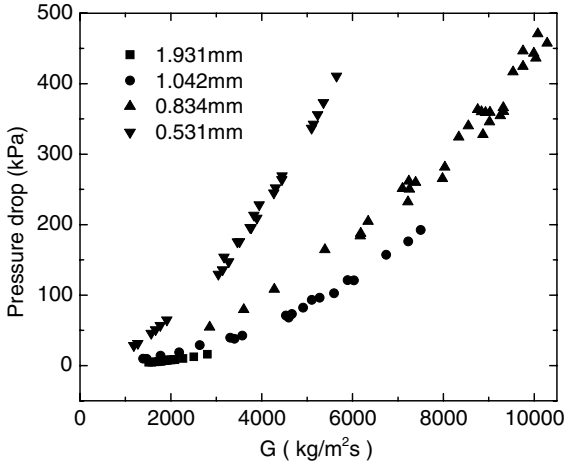

Fig. 3. Experimental results of the pressure drop at different mass fluxes.

even reaches nearly 500 kPa at $G = 10{,}000$ kg/m^{2}s, comparing to 380 kPa for the conventional channels with the same tube length and mass flux calculated by the Von Karman–Nikuradse correlation [20]. The possible reason is that the inner surface roughness of the drawing stainless steel tube becomes larger with the decrease of tube diameter due to the increase of manufacture complexity.

4.1.2. The surface roughness of the micro-tubes

Since the pioneering works by Darcy, Moody and Nikuradse, the surface roughness has been identified as a crucial parameter for the pressure drop of internal flow [20]. Usually, the surface roughness is represented by the average roughness ε or the relative surface roughness ε/D_i. For the conventional tubes, ε can be obtained from the tables given by Moody [21] according to the tube material and machining technique, and it is about 1.5 μm for the drawing stainless steel tube. However, this value still needs to be verified for the mini- and micro-channels. By using Acuor Alpha-step 500 surface profiler, the average roughness of the micro-tubes is measured, and the results are listed in Table 3. It is found that the average roughness increases as the tube diameter decreases, which indicates that the value given by Moody is no longer appropriate for the micro-tubes, at least for the present drawing tube with a diameter range of 0.5–2.0 mm. This large discrepancy may result from the fact that the shape and the size of roughness irregularities of the surface are significantly different from those of the commercial channels as the scale decreases.

4.1.3. The friction factor

To evaluate the importance of the relative surface roughness on the flow friction, the roughness Reynolds number is often used, which is defined as

$$Re_\varepsilon = Re\frac{\varepsilon}{D_i}\sqrt{f/8} \tag{12}$$

Table 3
The surface roughness of the micro-tubes

Number	Inner diameter D_i (mm)	Average roughness ε (μm)	Relative surface roughness ε/D_i
1	1.931	0.67	0.000347
2	1.042	0.86	0.000825
3	0.834	1.72	0.00206
4	0.531	2.31	0.00435

The flow can be divided into the hydraulically smooth, transitionally rough, and fully rough region according to the ranges of Re_ε:

$Re_\varepsilon < 5$ hydraulically smooth

$5 \leqslant Re_\varepsilon \leqslant 70$ transitionally rough

$Re_\varepsilon > 70$ fully rough

The friction factors of the single-phase liquid nitrogen in the micro-tubes are presented in Fig. 4. Obviously, all the data of the present experiments fall into the region below the line of $Re_\varepsilon = 70$, which means the flows are in the transitionally rough region characterized by the fact that the friction factor depends on both the Reynolds number and the relative surface roughness.

Moreover, the experimental friction factors are compared with the well-known correlations for the conventional channels in Fig. 4. The Von Karman-Nikuradse [20] correlation are used for the hydraulically smooth tube in the Reynolds number range from 4000 to 3×10^6:

$$\frac{1}{\sqrt{f}} = 0.868 \ln\left(\frac{1}{2} Re\sqrt{f}\right) - 0.198 \tag{13}$$

And the Colebrook [22] correlation is typically used for the Reynolds number between 4000 and 10^8

$$\frac{1}{\sqrt{f}} = -2.0 \log\left(\frac{\varepsilon/D_i}{3.7} + \frac{2.51}{Re\sqrt{f}}\right) \tag{14}$$

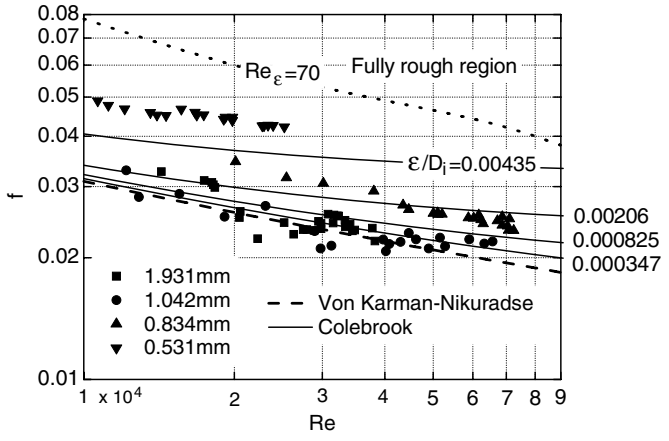

Fig. 4. Friction factors of the liquid nitrogen flow in the micro-tubes versus the Reynolds number.

Fig. 4 indicates that the friction factors for 1.931 and 1.042 mm tube agree quite well with the Von Karman–Nikuradse and Colebrook correlation. The difference between two correlations is very small because the relative surface roughness is so small that the tube can be considered as hydraulically smooth. However, as $\varepsilon/D_i = 0.00206$ for 0.834 mm tube, the relative surface roughness plays relatively important role on the friction factor. The Colebrook correlation can provide satisfactory predicted results, but the agreement with the Von Karman–Nikuradse correlation is poor, as shown in Fig. 4. For the tube with a diameter of 0.531 mm, the friction factor is by 20% higher than the result of the Colebrook correlation. The possible reason may be that the effect of roughness on fluid flow has not been completely understood, especially for the flow in the micro-channels. For example, Wu and Cheng [23] reported that the roughness plays an important role even in laminar flow region in micro-channels. However, the roughness does not affect the laminar flow in macro-channels. More recently, Taylor et al. [24] asserted that 3D surface assessment is required in metrology for the surface in micro-channels because one parameter, i.e., the average surface roughness, is not enough to describe the complete functionality of a surface.

Comparison of the measured friction factors for flow of liquid nitrogen in the micro-tubes with the Colebrook correlation is presented in Fig. 5. It can be seen that the Colebrook correlation can be basically used to predict the experimental friction factor although the effect of the roughness on the flow in micro-channels has not been understood completely. Nevertheless, the relative surface roughness of the micro-tubes must be measured accurately while using the Colebrook correlation to predict the friction factor for the micro-tubes, because it is apparently different with the conventional channels.

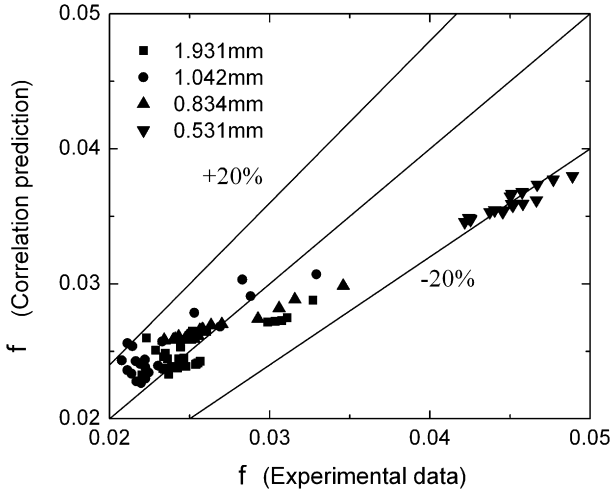

Fig. 5. Comparison of the measured friction factor for flow of liquid nitrogen in the micro-tubes with the Colebrook correlation.

4.1.4. The effect of heat flux on the mass flux and pressure drop

Stepped increase of heat flux can be realized through adjusting the DC power, while keeping other conditions in the system unchanged. Hence, the effect of heat flux on the mass flux and pressure drop is determined. Shown in Fig. 6 is one example for 0.531 mm tube. It can be seen that the pressure drop decreases apparently for higher heat flux. However, the mass flux almost remains constant. Other tubes also show similar trends. The result may be interpreted by the fact that the viscosity of liquid nitrogen decreases with the increase of the temperature. Hence, higher heat flux corresponds to higher temperature of liquid nitrogen, lower viscosity and lower pressure drop. The mass flux does not change for the density of liquid nitrogen is not sensitive to the heat flux.

4.2. Single-phase heat transfer

4.2.1. Local heat transfer characteristics

Figs. 7a and b show the variation of the temperature and heat transfer coefficient along 0.531 mm tube at a constant mass flux, 3272.8 kg/m^{2}s. In Fig. 7a, the fluid temperatures indicated by the dashed lines are calculated by Eq. (9). It can be seen that the local heat transfer coefficient decreases along the flow direction and also decreases with the increase of the heat flux. The heat transfer coefficient at the outlet is about 12.5% lower than that at the inlet for all three cases. This may result from the temperature dependence of the thermal conductivity of liquid nitrogen. As known that the heat conducted away from the wall, through the boundary sub-layer, equals to the heat transferred by convection:

$$-k_f \left.\frac{\partial T}{\partial y}\right|_{y=0} = h(T_w - T_f) \tag{15}$$

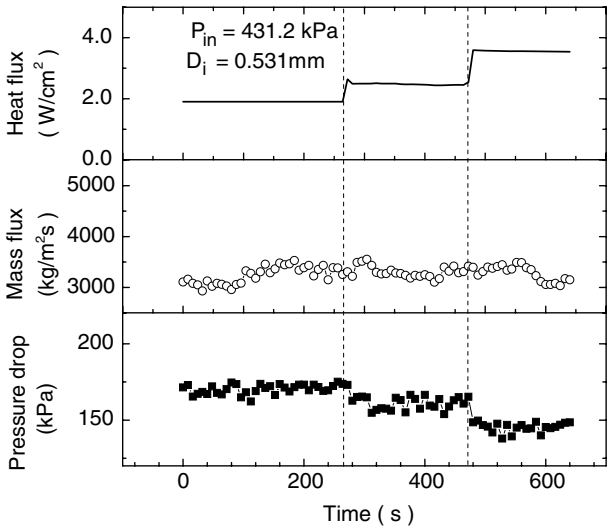

Fig. 6. The effect of heat flux on the mass flux and pressure drop for 0.531 mm tube.

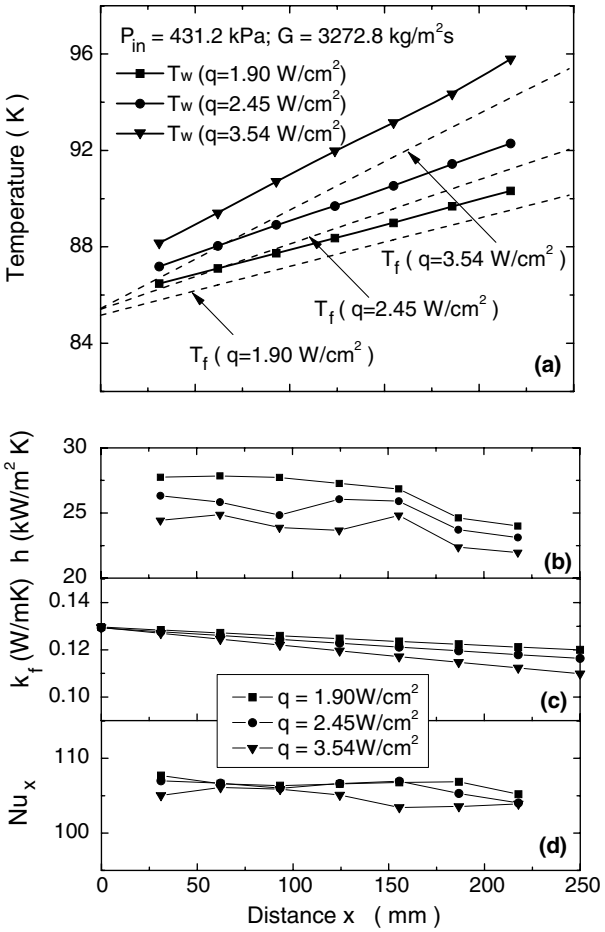

Fig. 7. Variation of the local heat transfer characteristics for 0.531 mm tube with different heat fluxes: (a) the wall temperature, (b) local heat transfer coefficient, (c) thermal conductivity of liquid nitrogen and (d) local Nusselt numbers.

So the thermal conductivity will have an important influence on convective heat transfer.

For the micro-tubes, the influence may be more significant because of the rapid increase of the fluid temperature along the micro-tube, which leads to the apparent variation of the thermal conductivity, as shown in Fig. 7c. It can be seen that the variation of the thermal conductivity shows similar tendency to the local heat transfer coefficient. This condition is also reported for the laminar flow by Herwig and Mahulikar [25], whose analysis shows the heat transfer coefficients differ by up to 30% depending on whether the property variation is accounted for or not. However, the variation trend is opposite to the present study. The main reason is that the thermal conductivity of liquid nitrogen drops with the increase of fluid temperature, which is similar to the refrigerants and opposite to water.

The effect of the thermal conductivity on heat transfer can be excluded by the dimensionless Nusselt number defined as Eq. (10). As shown in Fig. 7d, Nusselt number remains nearly constant, which indicates that the decrease of local heat transfer coefficient along the tube is mainly caused by the variation of thermal conductivity of liquid nitrogen with the temperature.

4.2.2. The average Nusselt number

The comparison between the experimental data and the correlations for the conventional channel, i.e. Dittus and Boelter [26] and Gnielinski [27] correlation, is shown in Fig. 8. Dittus–Boelter correlation for fully developed turbulent flow in smooth channels when $Re \geqslant 10{,}000$ is

$$Nu = 0.023 Re^{0.8} Pr^{0.4} \tag{16}$$

And Gnielinski correlation can be used for $3000 < Re < 5 \times 10^6$

$$Nu = \frac{(f/8)\cdot(Re - 1000)Pr}{1 + 12.7\sqrt{f/8}(Pr^{2/3} - 1)} \tag{17}$$

where the friction factor for smooth pipe is usually given by

$$f = (1.82\log(Re) - 1.64)^{-2} \tag{18}$$

From Fig. 8, it can be seen that the experimental Nusselt numbers are higher than those predicted by Dittus–Boelter and Gnielinski correlations. The deviation becomes more significant with the decrease of tube diameter. The smaller the tube diameter is, the higher the Nusselt number is for the same Reynolds number. For the 0.531 mm tube, the experimental Nusselt numbers even double those predicted by Eqs. (16) and (17).

In fact, the flow friction factors of liquid nitrogen flow in the present micro-tubes are different from those of the conventional channels according to the analysis presented in Section 4.1. Therefore, for the micro-tubes, the Gnielinski correlation must be modified by replacing Eq. (18) with the Colebrook correlation, i.e. Eq. (14). It should be noted that the corresponding relative surface roughness of the micro-tubes must be used in Colebrook correlation. As shown in Fig. 8, the experimental Nusselt numbers agree well with the predicted values by the modified Gnielinski correlation. The mean absolute error (MAE) defined as below is about 6.4%

$$\mathrm{MAE} = \frac{1}{M}\sum \frac{|Nu_{\mathrm{exp}} - Nu_{\mathrm{pred}}|}{Nu_{\mathrm{exp}}} \times 100\% \tag{19}$$

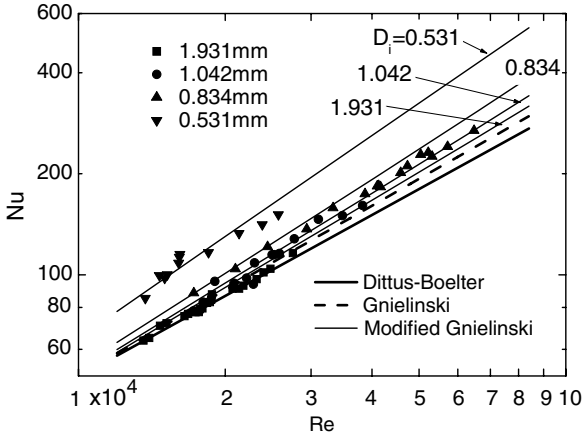

Fig. 8. Comparison of the experimental Nusselt numbers with the correlations for the conventional channels.

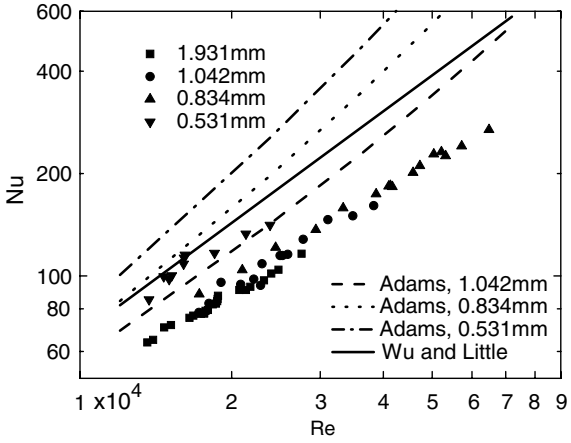

Fig. 9. Comparison of the experimental Nusselt numbers with the correlations for the micro-channels.

where M is the number of the experimental data. Hence, it is suggested that the large surface roughness may influence the turbulent flow and result in high friction factor, meanwhile, improve heat transfer performance.

The experimental Nusselt numbers are further compared, in Fig. 9, with the results from the correlations used for the micro-channels. The correlations include Wu and Little [6] correlation for $Re > 3000$:

$$Nu = 0.0022 Re^{1.09} Pr^{0.4} \tag{20}$$

and Adams et al. [7] correlation

$$Nu_{\mathrm{Adams}} = Nu_{\mathrm{Gnielinski}}(1 + F) \tag{21}$$

where $F = 7.6 \times 10^{-5} \cdot Re \cdot (1 - (D_i/D_r)^2)$, $D_r = 1.161$ mm and the Reynolds number ranges from 2.3×10^3 to 2.3×10^4. It can be seen that the predicted results from Wu and Little [6] correlation are nearly equal to the experimental Nusselt number for the 0.531 mm tube, but much higher than those for other three tubes. The divergence might result from the fact that the correlation is derived from the data of nitrogen gas.

The results from Adams et al. [7] show similar trends to the present data, i.e., the decrease of tube diameter results in higher Nusselt numbers. However, the present experimental Nusselt numbers are lower than those predicted by Adams et al. [7]. The possible reason may be that the test tubes are machined in different methods. Adams' flow passages were produced by the electrode discharge machining (EDM) technique, so the relative surface roughness might be higher than that of the drawing tubes used in present experiments [28]. However, Adams et al. [7] did not report the surface roughness and friction factor in their paper.

5. Conclusions

The flow and heat transfer characteristics of liquid nitrogen in the micro-tubes are investigated experimentally. The following conclusions can be drawn:

(1) The friction factor for liquid nitrogen flow in the micro-tubes is higher than the value predicted by the correlations used for the conventional channels. The Colebrook correlation must be modified by the measured surface roughness of the micro-tubes to predict the single-phase friction factor of liquid nitrogen flow in the micro-tubes.
(2) The variation of thermal properties of liquid nitrogen, i.e., viscosity and thermal conductivity, with temperature has important influence on the flow and heat transfer characteristics of liquid nitrogen in the micro-tubes. In details, with the increase of liquid nitrogen temperature, the pressure drop decreases as a result of lower viscosity. Contrary to water, the local heat transfer coefficient decreases along the flow direction and also decreases with the increase of the heat flux. The main reason is that the thermal conductivity of liquid nitrogen is inversely proportional to temperature.
(3) The average Nusselt numbers for the micro-tubes are higher than the results predicted by Dittus–Boelter and Gnielinski correlations applicable to the conventional channels, and they increase with the decrease of the tube diameter. Large surface roughness of the micro-tube can improve the heat transfer performance. Taking into account the effect of the surface roughness, the modified Gnielinski correlation can accurately predict the present experiments data. The correlations for the micro-channels overestimate the average Nusselt number with large deviation, which may result from different channel surface functionalities decided by different machining techniques.

Acknowledgements

This research is jointly supported by A Foundation for the Author of National Excellent Doctoral Dissertation of PR China (200236), National Natural Science Foundation of China (50306014, 50436030) and NCET.

References

[1] P. Wu, W.A. Little, Measurement of friction factors for the flow of gases in very fined channels used for microminiature Joule–Thompson refrigerators, Cryogenics 23 (5) (1983) 272–277.
[2] S. Lin, C.K. Kwok, R.Y. Li, Z.H. Chen, Z.Y. Chan, Local frictional pressure during vaporization of R-12 through capillary tubes, Int. J. Multiphase Flow 17 (1) (1991) 95–102.
[3] S.S. Hsieh, C.Y. Lin, C.F. Huang, H.H. Tsai, Liquid flow in a microchannel, J. Micromech. Microeng. 14 (4) (2004) 436–445.
[4] B. Agostini, B. Watel, A. Bontemps, B. Thonon, Liquid flow friction factor and heat transfer coefficient in small channels: an experimental investigation, Exp. Therm. Fluid Sci. 28 (2–3) (2004) 97–103.
[5] C.Y. Yang, J.C. Wu, H.T. Chien, S.R. Lu, Friction characteristics of water, R-134a, and air in small tubes, Microscale Thermophys. Eng. 7 (4) (2003) 335–348.
[6] P. Wu, W.A. Little, Measurement of the heat transfer characteristics of gas flow in fine channel heat exchangers used for microminiature refrigerators, Cryogenics 24 (8) (1984) 415–420.
[7] T. M Adams, S.I. Abdel-Khalik, S.M. Jeter, Z.H. Qureshi, An experiment investigation of single-phase forced convection in microchannels, Int. J. Heat Mass Transfer 41 (6–7) (1998) 851–857.
[8] G.R. Warrier, V.K. Dhir, L.A. Momoda, Heat transfer and pressure drop in narrow rectangular channels, Exp. Therm. Fluid Sci. 26 (1) (2002) 53–64.
[9] W. Owhaib, B. Palm, Experimental investigation of single-phase convective heat transfer in circular microchannels, Exp. Therm. Fluid Sci. 28 (2–3) (2004) 105–110.
[10] B.X. Wang, X.F. Peng, Experimental investigation on liquid forced-convection heat transfer through micro-channels, Int. J. Heat Mass Transfer 37 (1) (1994) 73–82.
[11] X.F. Peng, G.P. Peterson, The effect of thermofliud and geometrical parameters on convection of liquid through rectangular microchannels, Int. J. Heat Mass Transfer 38 (4) (1995) 755–758.
[12] Z.Y. Guo, Z.X. Li, Size effect on microscale single-phase flow and heat transfer, Int. J. Heat Mass Transfer 46 (1) (2003) 149–159.
[13] G.L. Morini, Single-phase convective heat transfer in microchannels: a review of experimental results, Int. J. Therm. Sci. 43 (7) (2004) 631–651.
[14] V.N. Pavlov, Development of perspective cryogenic surgical apparatus, Cryogenics 40 (6) (2000) 361–363.
[15] X.D. Zhou, Z.Y. Tang, Y.Q. Yu, Clinical evaluation of cryosurgery in the treatment of primary liver cancer, Cancer 61 (10) (1988) 1889–1892.
[16] J. Baust, A.A. Gage, H. Ma, C.M. Zhang, Minimally invasive cryosurgery – technological advances, Cryobiology 34 (4) (1997) 373–384.
[17] M.O. Maiwand, J.M. Evans, J.E. Beeson, The application of cryosurgery in the treatment of lung cancer, Cryobiology 48 (1) (2004) 55–61.
[18] J.C. Saliken, B.J. Donnelly, J.C. Rewcastle, The evolution and state of modern technology for prostate cryosurgery, Urology 60 (Suppl. 1) (2002) 26–33.
[19] R. Span, E.W. Lemmon, R.T. Jacobsen, W. Wagner, A. Yokoziki, A reference equation of state for the thermodynamic properties of nitrogen for temperatures from 63.151 to 1000 K and pressures to 2200 MPa, J. Phys. Chem. Ref. Data 29 (6) (2000) 1361–1433.
[20] F.M. White, Fluid Mechanics, third ed., McGraw-Hill, New York, 1994, pp. 307–320.
[21] L.F. Moody, Friction factors for pipe flow, Trans. ASME 66 (1944) 671–683.
[22] C.F. Colebrook, Turbulent flow in pipes, with particular reference on the transition between the smooth and rough pipe laws, J. Inst. Civ. Eng. Lond. 11 (4) (1939) 133–156.
[23] H.Y. Wu, P. Cheng, An experimental study of convective heat transfer in silicon microchannels with different surface conditions, Int. J. Heat Mass Transfer 46 (14) (2003) 2547–2556.
[24] J.B. Taylor, A.L. Carrano, S.G. Kandlikar, Characterization of the effect of surface roughness and texture on fluid flow-past, present, and future, Int. J. Therm. Sci. 45 (10) (2006) 962–968.
[25] H. Herwig, S.P. Mahulikar, Variable property effects in single-phase incompressible flows through microchannels, Int. J. Therm. Sci. 45 (10) (2006) 977–981.
[26] F.W. Dittus, L.M.K. Boelter, Heat transfer in turbulent pipe and channel flow, Univ. Califoria, Berkeley, Publ. Eng. 2 (13) (1930) 443–461.
[27] V. Gnielinski, New equations for heat transfer in turbulent pipe and channel flow, Int. Chem. Eng. 16 (1976) 359–368.
[28] F. Han, M. Kunieda, Development of parallel spark electrical discharge machining, Precis. Eng. 28 (1) (2004) 65–72.